Eur Biophys J (1996) 24: 185–193

European Biophysics Journal

Distance distributions from the tyrosyl to disulfide residues in the oxytocin and [Arg^8]-vasopressin measured using frequency-domain fluorescence resonance energy transfer

Henryk Szmacinski [1], **Wieslaw Wiczk** [1], **Mayer N. Fishman** [1], **Peggy S. Eis** [1], **Joseph R. Lakowicz** [1], **Michael L. Johnson** [2]

[1] Center for Fluorescence Spectroscopy and Department of Biological Chemistry, School of Medicine, University of Maryland at Baltimore, Baltimore, MD 21201, USA
[2] University of Virginia, Department of Pharmacology, Charlottesville, VA 22908, USA

Received: 16 October 1994 / Accepted: 23 October 1995

Abstract. We have examined the fluorescence intensity decays of oxytocin and [Arg^8]-vasopressin resulting from the single tyrosyl residue in each peptide, and the intensity decay of the Asu^{1,6}-analogues in which the disulfide bridge is substituted by a CH_2-CH_2 bridge. Viscosity-dependent steady state and intensity decay measurements indicated that fluorescence resonance energy transfer (FRET) from tyrosyl phenol to the disulfide bridge is responsible for the decrease in fluorescence relative to the Asu-analogues. The frequency-domain phase and modulation data for the tyrosyl donor were interpreted in terms of fluorescence resonance energy transfer (FRET) to the weakly absorbing disulfide bridge and a distribution of donor-to-acceptor distances. Energy transfer efficiencies were determined from both time-resolved and steady-state measurements. Fitting the frequency-domain phase and modulation data to a Gaussian distance distribution indicated that the average inter-chromophoric distance (R_{av}) is similar in both compounds, $R_{av}=7.94$ Å for oxytocin and $R_{av}=8.00$ Å for vasopressin. However, the width of the distance distribution is narrower for vasopression (hw = 2.80 Å) than for oxytocin (hw = 3.58 Å), which is consistent with restriction of the tyrosine phenol motion due to its stacking with the Phe^3 side chain of vasopressin. Finally, the recovered distance distribution functions are compared with histograms describing the distance between the chromophores during the course of long, *in vacuo,* molecular dynamics runs using the computer program CHARMm and the QUANTA 3.0 parameters.

Key words: Fluorescence – Energy transfor – Oxytocin – Vasopressin – Distance distribution – Time-resolved fluorescence – Frequency-domain fluorescence

Abbreviations: AVP, [Arg^8]-vasopressin; FRET, fluorescence resonance energy transfer; FD, frequency-domain; D, donor; A, acceptor; DTT, dithiothreitol

Correspondence to: J. R. Lakowicz

Introduction

The conformation and dynamics of oxytocin and vasopressin in solution are of interest to understand their different physiological effects of stimulating smooth muscle contractions or as an antidiuretic, respectively. The conformation of these peptides has been studied using molecular mechanics (Liwo et al. 1988), X-ray crystallography (Langs et al. 1986; Husain et al. 1990), NMR (Glickson et al. 1972; Brewster and Hruby 1973; Krauss and Cowburn 1981), as well as steady-state (Cowgill 1964, 1967; Chen 1967; Bodanszky et al. 1981; Laws et al. 1986; Ross et al. 1986a; Swadesh et al. 1987) and time-resolved fluorescence of the intrinsic tyrosine emission (Laws et al. 1986; Ross et al. 1986a). Ross et al. (1986a) interpreted the fluorescence measurements of oxytocin in terms of structured features of the peptide conformation. These workers (Ross et al. 1986a) interpreted the multi-exponential tyrosine intensity decays of oxytocin and its Asu-analog in terms of three tyrosine C_α-C_β rotational isomers. In the Asu-analogues the disulfide bridge is replaced by a CH_2-CH_2 bridge. The chemical structures are shown in Scheme I. The decrease in fluorescence yield for the native hormone compared to the Asu-analog was ascribed to one of the multi-exponential intensity decay components, corresponding to one of the rotational isomers, as being quenched due to a rotational-position specific interaction between the tyrosyl residue and the disulfide group. Previous studies have revealed the general conformational features of oxytocin and vasopressin, and provide a useful foundation for the interpretation of the present time-resolved data. In particular, NMR measurements have indicated that oxytocin is conformationally flexible in solution (Brewster and Hruby 1973), and that the backbone structures of Lys^8-vasopressin and oxytocin differ (Glickson et al. 1972). A thin film dialysis technique indicated that Lys^8-vasopressin has a more extended conformation than oxytocin (Craig et al. 1964). Consistent with this dialysis result, others have reported (Krauss and Cowburn 1981), that there is no association of the tripeptide (residues 7–8–9) of oxytocin with the ring (residues 1–6).

Analysis of the X-ray crystal structures of oxytocin and it analogues (Husain et al. 1990) revealed a "disordered" state in the disulfide bond region, suggesting that a variety of conformations would exist in solution.

In addition to time-resolved fluorescence measurements (Ross et al. 1986 a), there have been several studies examining the steady-state intensity of oxytocin. The quantum yield of oxytocin is significantly less than its Asu-analogue, 0.025 and 0.066 in water at 25 °C (Bodanszky et al. 1981), and 0.024 and 0.091 in buffer pH 3 at 5 °C, respectively (Ross et al. 1986 a). Cowgill (1964) ruled out quenching by the disulfide bond as the origin of the decreased quantum yield based on the unchanged intensity when the disulfide is reduced with mercaptoethanol. Cowgill (1967) ascribed the diminished fluorescence to vibrational dissipation of energy, not collisional quenching, hydrogen-bond formation or FRET. Bodanszky et al. (1981) suggested that the effect of the disulfide group is masked by the change in tyrosine emission due to the change of environment that occurs upon reduction of the disulfide bond. However, based on steady-state data the mechanisms and stearic requirements of disulfide quenching could not be deduced. Swadesh et al. (1987) ruled out collisional quenching based on a Stern-Volmer analysis and suggested the formation of a complex between tyrosyl and cystine residues. They have not excluded other quenching mechanisms but long range energy transfer as a reason for the intramolecular quenching has not been considered. Quenching mechanisms of tyrosine in polypeptides and proteins has been recently reviewed by Ross et al. (1992). Considerable effort has been made to understand the mechanism of disulfide quenching but still there is no conclusive picture.

In the present paper we describe a different interpretation of the time-dependent intensity decays of oxytocin and vasopressin. We interpreted the decreased lifetime and increased heterogeneity of the tyrosine decays of these native peptides, relative to the Asu-analogues, as due to fluorescence resonance energy transfer (FRET) from tyrosine to the disulfide acceptor. The frequency-domain (FD) intensity decays data are interpreted in terms of the distance distribution between the tyrosine donors and the disulfide acceptors. An advantage of the time-resolved FRET measurements is its ability to reveal the conformational heterogeneity, in terms of a range of donor (tyrosyl) to acceptor (disulfide) distances. Energy fransfer from tyrosine to disulfide bridge as a quenching mechanism has been already proposed by Shafferman and Stein (1974). Reduced tyrosine fluorescence has not been considered by other researchers because the efficiency of quenching near 60% appeared to be too high for energy transfer given the weak cysteine absorption which overlaps the fluorescence of tyrosine. In these studies it was very difficult to distinguish energy transfer from static quenching process. Usually, the tyrosine has been regarded as a donor for other acceptors, like tyrosine, phenylalanine, and tryptophan (Eisinger 1969; Eisinger et al. 1969).

Theory

Time-resolved fluorescence

The frequency-domain intensity decay measurements were initially analyzed using the multi-exponential model

$$I(t) = \sum_i \alpha_i \exp\left(-\frac{t}{\tau_i}\right) \tag{1}$$

where α_i are the pre-exponential factors, τ the decay times, and $\Sigma\alpha_i = 1.0$. In the present paper, the purpose of this analyses is to obtain a parametrized form for the donor decay for subsequent use in the distance distribution analysis. In our case, the intensity decays of the Asu-analogues (donors) are not single exponentials. The values of τ_i and α_i can be determined by nonlinear least-squares fitting, as described previously in detail (Lakowicz et al. 1984; Gratton et al. 1984). The goodness-of-fit is determined by the value of the reduced chi-square

$$\chi_r^2 = \frac{1}{\nu}\left(\frac{\theta_\omega - \theta_{\omega c}}{\Delta\theta}\right)^2 + \frac{1}{\nu}\left(\frac{m_\omega - m_{\omega c}}{\Delta m}\right)^2 \tag{2}$$

where the subscript ω indicates the modulation frequency, the subscript c indicates the calculated values of the phase angle (θ) or the modulation (m) for some assumed values of τ_i and α_i $\Delta\theta$ and Δm are the experimental uncertainties in the measured values of the phase and modulation, and υ is the number of degrees of freedom.

The theory for frequency-domain measurements of energy transfer to recover distance distributions has been described previously in detail (Lakowicz et al. 1988). For a single exponential decay of the donor it is known that the rate of energy transfer is proportional to the decay rate, or inversely proportional to the lifetime. The intensity decays of the Asu-analogues (donors) were found to be double-exponential. Assuming the model of tyrosine C_α-C_β rotational isomers (Laws et al. 1986; Ross et al. 1986 a) the energy transfer rates for each component are inversely proportional to the respective decay time. Hence, the transfer rate for each component i in the decay is given by

$$k_{DAi} = \frac{1}{\tau_{Di}}\left(\frac{R_0}{r}\right)^6 \tag{3}$$

when r is the donor-to-acceptor distance, R_0 is the Förster distance (Förster 1948), and τ_{Di} is the decay time of the i'th component of the donor measured in the absence of acceptor. In the present paper the donor decay without acceptor is obtained from the Asu-analogues.

The decay times of the donor are decreased by fluorescence resonance energy transfer (FRET). Assuming that FRET is the only additional mechanism affecting the tyrosyl decays in the native peptides compare to the Asu-analogues, the tyrosyl decay times are given by

$$\frac{1}{\tau_{DAi}} = \frac{1}{\tau_{Di}} + \frac{1}{\tau_{Di}}\left(\frac{R_0}{r}\right)^6. \tag{4}$$

In the present paper the pepties are assumed to be conformationally flexible, and thus display a range of tyrosyl do-

nor (D) to disulfide acceptors (A) distances. For those peptides with a given D- to -A distance r the intensity decay is given by

$$I_{DA}(r,t) = \sum_i \alpha_{Di} \exp\left[-\frac{t}{\tau_{Di}} - \frac{t}{\tau_{Di}}\left(\frac{R_0}{r}\right)^6\right]. \quad (5)$$

The intensity decay for the ensemble of D-A pairs is given by

$$I_{DA}(t) = \int_0^\infty P(r)\, I_{DA}(r,t)\, dr \quad (6)$$

where P(r) is the probability distribution of distances. In the present work, we assume the distance probability distribution is a Gaussian function

$$P(r) = \frac{1}{\sigma\sqrt{2\pi}} \exp\left[-\frac{1}{2}\left(\frac{r - R_{av}}{\sigma}\right)^2\right] \quad (7)$$

where R_{av} is the mean distance and σ represents the standard deviation of the untruncated Gaussian. The standard deviation is related to the half-width (hw, full width at half-maximum height) by $hw = 2.354\sigma$. The values of R_{av} and hw are determined using Eq. (6) by nonlinear least-squares similar to that described by Eq. (2) for a multi-exponential intensity decay (Lakowicz et al. 1988, 1990a; Cheung et al. 1991a, b). This analysis requires the use of two frequency-domain intensity decays, one for the donor alone (Asu-analogue) and one for the D-A pair (-S-S-peptide). The values of α_{Di} and τ_{Di} from the Asu-analogue are fixed parameters in the distance distribution analysis. In the present analysis we do not consider the effects of donor-to-acceptor diffusion (Lakowicz et al. 1991a, b; Kusba and Lakowicz 1994), which is not expected to be significant in the time scale of the tyrosyl decays.

Molecular dynamics calculations

A molecular dynamics conformational survey was used to provide an independent estimate for the distance distribution. The initial conformation of each hormone was based on the published crystal structure for pressinoic acid (i.e. residues 1–6 of vasopressin, Langs et al. 1986). After a short "equilibration run" 1500 survey steps were recorded. The program CHARMm with the parameter set from QUANTA 3.0 (Polygen Corp.) was used with only the polar hydrogens explicitly represented. The dipolar attraction function used a constant dielectric with $\varepsilon = 1$; the default tolerance on the temperature window was used.

Each survey step consisted of 300×1 ps steps at simulation temperature T = 1200 °K then 200×1 ps steps of "cooling down" to T = 300 °K then 200×1 ps steps of "equilibration" at T = 300 °K. At this point the distance between the center of the phenol ring and the middle of the disulfide bridge was recorded as well as some bond angle information. The starting conformation for each subsequent step was the one from the end of the T = 1200 °K section of the previous one. The purpose of the high temperature cycle was to increase the rate of conformational transitions so that the sample would not be restricted to the vicinity of the previous conformation.

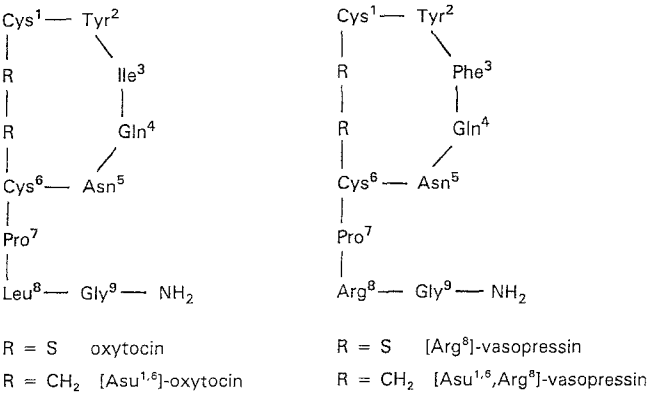

Scheme I. Structures of oxytocin [Arg^8]-vasopressin, and their Asu analogues

Materials and methods

The hormones (oxytocin and [Arg^8]-vasopressin) and their Asu^{1,6}-analogues were obtained from Bachem (Torrance, CA). Their purity was checked by HPLC using an analytical Vydac C_{18} column and 0.1% trifluoracetic acid (TFA) in water and 0.1% TFA in acetonitrile as eluents. The structures of hormones and their Asu^{1,6}-analogues are shown in Scheme I.

Steady-state spectra were obtained on a SLM 8000 fluorometer with a 4 nm bandwidth for excitation and an 8 nm bandwidth for emission. The excitation wavelength was 287 nm. The quantum yields were measured relative to a value of 0.14 for tyrosine in water at 20 °C (Chen 1967). The samples were prepared in 10 mM MOPS buffer pH 7.0, and in propylene glycol. Additionally, the oxytocin and [Asu^{1,6}] were prepared in buffer with pH 3.1, where only one chemical (ionic) form is expected in solution.

Time-resolved measurements were performed on the frequency-domain fluorometer described in (Lakowicz et al. 1986). The emission was observed through a 300 nm interference filter (10 nm bandwidth).

Results and discussion

As will be shown below, the presence of a disulfide group reduces the tyrosyl quantum yield and lifetime of oxytocin and vasopression. We reasoned that several mechanisms could account for quenching by the disulfide group. The disulfide group could act as a collisional quencher, which requires molecular contact and is strongly dependent on solvent viscosity. This quenching could be static, which should be independent of the solvent viscosity. Alternatively, the disulfide bridge (Cys^1–Cys^6) could act as a FRET acceptor, which is a through space interaction and does not require molecular contact. We performed experiments to evaluate these three possible mechanisms for quenching of the fluorescence of the tyrosine residues. Altering the solvent viscosity allows the effect of static and dynamic quenching to be compared. When viscosity is low, both static and dynamic quenching may occur. When the viscosity is high, dynamic quenching is decreased whereas

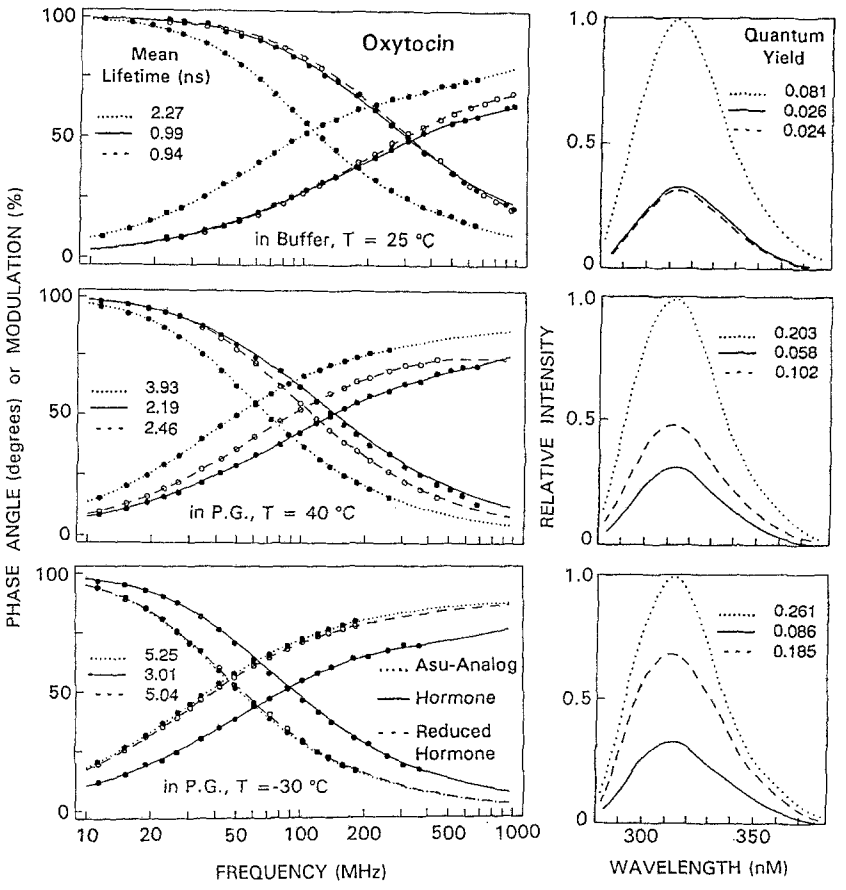

Fig. 1. Viscosity-dependent frequency-domain intensity decays (*left*) and steady-state (*right*) measurements for oxytocin. Data are shown for the native hormone (——), reduced hormone (- - - -), and Asu-analogue (.....) in buffer (*top*), in propylene glycol at 40 °C (*middle*) and in propylene glycol at −30 °C (*bottom*)

static quenching is unaffected. FRET is not expected to change significantly due to changes in viscosity. While FRET occurs on the nanosecond timescale, it is a through space interaction which does not require diffusive motion to occur. The extent of FRET can be affected by the rate of diffusion, such effects are expected to be modest on the time scale of the tyrosyl intensity decay. In the present paper we take dynamic quenching to mean a collisional quenching processes which requires diffusion, but is not due to the FRET mechanism.

To distinguish the role of each mechanism we analyzed both steady state (quantum yield) and frequency-domain intensity decay measurements. Each hormone was measured without dithiothreitol (DTT) (native hormone) and with 20 mM DTT for reduction of the disulfide bridge (reduced hormone). The measurements were performed in aqueous buffers and in a more viscous solutions of propylene glycol. The viscosity of propylene glycol was changed by variations in temperature. The magnitude of tyrosyl fluorescence quenching of native and reduced hormones were examined relative to their respective Asu-analogues at the same experimental conditions. The data are presented in Fig. 1 for oxytocin and in Fig. 2 for AVP. For concise presentation, data at two viscosities of propylene glycol are presented and discussed, low viscosity, 17 cP (40 °C) and high viscosity, over 2500 cP (−30 °C). The left panels of Figs. 1 and 2 show frequency-domain intensity decay data (points) and the best fit of multi-exponential model (lines, Eq. (1)). The detailed intensity decay analyses for oxytocin and AVP in aqueous buffers are summarized in Table 1.

We used the multi-exponential analysis to calculate the mean lifetimes in order to estimate quenching from the FD measurements for comparison with those from steady-state measurements (right panel of Figs. 1 and 2). It should be noted that the decrease of quantum yield is equal to decrease of mean lifetime if only collisional quenching occurs. In the presence of static quenching the decay time constants are not affected, a change of mean lifetime is not observed, but the quantum yield is reduced. FRET usually reduces the mean lifetime, but often with a smaller decrease of mean lifetime compared to the decrease in quantum yield. The data presented in Figs. 1 and 2 show higher quenching observed from the relative quantum yields than from the relative mean lifetimes for each case.

In aqueous buffer (Figs. 1 and 2, top) there were no significant differences in the amount of quenching of the native and reduced hormones (with DTT), observed from either the time-resolved or steady-state measurements. The steady-state data are in agreement with earlier observations (Cowgill 1964). It is also important to note that intensity decays are very similar for the native and reduced hormones. Such indistinguishable quenching of native and reduced hormones observed either from steady-state or time-resolved measurements very likely clarify the difficulties to assign the quenching mechanism of tyrosyl residue in the native hormones (Cowgill 1967; Ross et al. 1986a; Swadesh et al. 1987).

Increased viscosity of the solvent (P. G. at various temperatures from 40 °C to −30 °C) resulted in decreased quenching of the reduced hormones observed from the

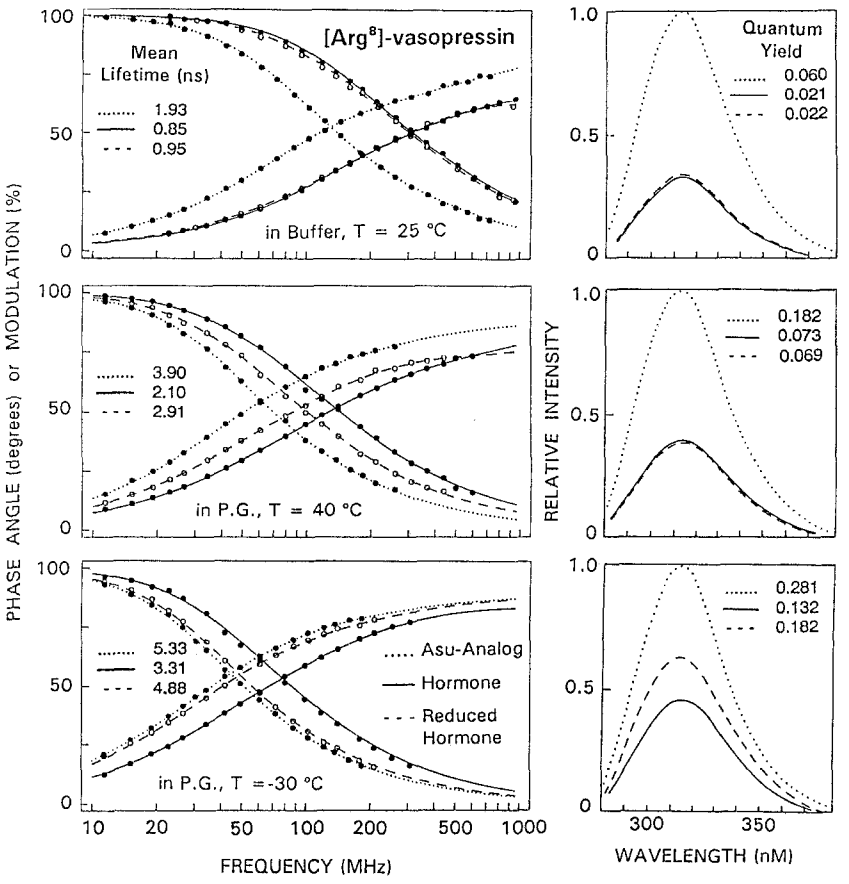

Fig. 2. Viscosity-dependent frequency-domain intensity decays (*left*) and steady-state (*right*) measurements of vasopression. Data are shown for the native hormone (——), reduced hormone (----), and Asu-analogue (.....) in buffer (*top*), in propylene glycol at 40 °C (middle) and in propylene glycol at –30 °C (*bottom*)

Table 1. Multi-exponential analysis of [Arg^8]-vasopressin and oxytocin and their Asu^{1,6}-analogues in 10 mM MOPS buffer pH 7.0, at 25 °C, $\lambda_{exc}=287$ nm, $\lambda_{obs}=301$ nm

Compound	τ_i (ns)	α_i	f_i[a]	$\bar{\tau}$(ns)[b]	$\chi^2_R(1)$	(2)	(3)[c]
Asu^{1,6}Arg^8-vasopressin	0.37	0.361	0.091				
	2.09	0.639	0.909	1.93	287.6	2.6	–
Arg^8-vasopressin	0.03	0.453	0.030				
	0.42	0.346	0.371				
	1.16	0.200	0.599	0.85	432.8	15.5	2.9
Arg^8-vasopressin + 20 mm DTT	0.03	0.600	0.058				
	0.58	0.276	0.454				
	1.39	0.124	0.488	0.95	578.2	18.7	3.4
Asu^{1,6}-oxytocin	0.36	0.369	0.080				
	2.43	0.631	0.920	2.27	354.2	2.0	–
Oxytocin	0.06	0.496	0.068				
	0.55	0.366	0.452				
	1.54	0.138	0.480	0.99	894.2	32.4	3.2
Oxytocin + 20 mM DTT	0.01	0.648	0.030				
	0.53	0.248	0.466				
	1.38	0.104	0.504	0.94	322.5	10.6	2.2
Asu^{1,6}-oxytocin[d]	0.26	0.380	0.061				
	2.45	0.620	0.939	2.32	143.1	2.0	–
Oxytocin[d]	0.08	0.432	0.074				
	0.46	0.379	0.374				
	1.37	0.189	0.552	0.93	342.8	6.0	1.4

[a] Fractional intensity $f_i=\alpha_i\tau_i/\Sigma\alpha_j\tau_j$
[b] Mean lifetime $\bar{\tau}=\Sigma f_i\tau_i$
[c] Number of components in multi-exponential analysis
[d] In 10 mM MOPS buffer pH 3.1

time-resolved (mean lifetimes) and from steady state measurements. The data for two temperatures are presented in Figs. 1 and 2 (dashed lines). At high viscosity (–30 °C), where dynamic quenching has been minimized only minor quenching (less than 8%) was observed from the FD measurement. However, there is substantial quenching seen from the steady state intensity (about 30%). The combined, FD and steady state intensity data can be interpreted as an evidence of collisional and static quenching of tyrosyl fluorescence by the reduced disulfide bonds. Our steady-state data for the reduced hormones extends the studies by Swadesh et al. (1987) over a larger viscosities range where the collisional quenching could be distinguished from the complexational (static).

For the native hormones, viscosity independent and similar quenching observed from FD and intensity data can be explained as a FRET from tyrosyl residue to the disulfide bridge. Additionally, more heterogenious intensity decays of native hormones relative to their respective Asu-analogues, can be likely a result of distance distribution between tyrosyl (donor) and disulfide bridge (acceptor).

Assuming the slow-exchange rotamer model for oxytocin (Laws et al. 1986; Ross et al. 1986a) the complex intensity decays can be regarded as a result of interactions of three tyrosine rotamers with the disulfide bridge. The best approach would be to recover a multicomponent distance distribution. However, to correlate the rotamer populations with the decay time amplitudes requires global analysis and the linked-function approach (Ross et al. 1986b), where the analysis of intensity decay is restricted by linking the amplitudes with proton NMR-determined rotamer populations. Nevertheless, reasonable comparison can be made between amplitudes (α_i) determined from FD measurements and rotamer populations (p_i) published by Ross et al. (1986a) for oxytocin and its Asu-analogue assuming that the shortest decay time to be associated with rotamer population p_{II} (Laws et al. 1986). Thus, for oxytocin (Table 1, pH 7 and Ross et al. 1986a), $\alpha_1 = 0.496$ should represent p_{II} (0.39), $\alpha_2 = 0.366$ reflects p_I (0.48), and $\alpha_3 = 0.138$, p_{III} (0.12). Double-exponential intensity decay for $Asu^{1,6}$-oxytocin can be explained that the population p_{III} is small (0.08) and decay times for p_I and p_{III} are comparable (Ross et al. 1986a). Very similar intensity decay heterogeneity was observed for oxytocin in buffer at pH 7.0 and 3.1 (Table 1) which indicate that the tyrosyl residue in oxytocin did not undergo excited-state proton transfer under our experimental conditions. Direct comparison of decay times of $Asu^{1,6}$-oxytocin (donor) with oxytocin (donor-acceptor) showed that rotamer II is quenched the most (from 0.36 to 0.06 ns) and rotamer III the least (from 2.43 to 1.54 ns). However, such comparison should be considered as an approximation since the intensity decay of each rotamer population in the presence of FRET should be described by a non-exponential decay. The measured intensity decays for native hormones are the average of a more complex decays from the three rotamer populations. It is known that most of complex intensity decays can be well fitted by three-exponential model with five independent parameters (Eq. (1)).

In our analysis of distance distribution we used intensity decay of native hormones to fit the Eq. (6) where the donor is represented by the double exponential intensity decays (e.g. two rotamer populations) of the Asu-analogues assuming the same distance distribution for both populations.

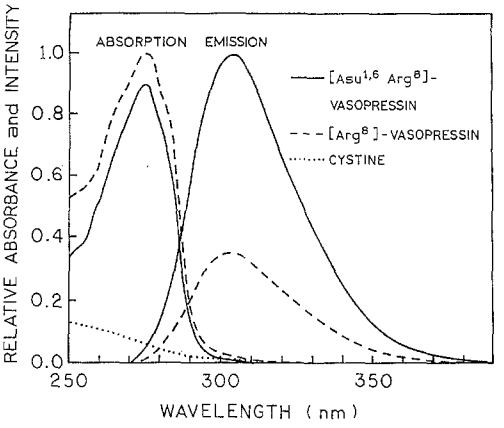

Fig. 3. Absorption and emission spectra of Arg^8-vasopressin (----), its $Asu^{1,6}$-analog (——), and absorption spectrum of cystine (.....) in the buffer at 25 °C. Spectra for oxytocin and Asu-oxytocin were similar (*not shown*)

Assuming that the energy transfer is due to the Förster mechanism, we calculated the Förster distances for energy transfer (R_0) using the absorption spectrum of cystine ($\varepsilon = 160\ M^{-1}\ cm^{-1}$ at 275 nm), or the difference absorption spectrum (hormone minus Asu-analog, $\varepsilon = 206\ M^{-1}\ cm^{-1}$ at 275 nm) as the absorption spectrum of the acceptor, and the experimentally determined emission spectrum and quantum yields of the Asu-analogues. The absorption and emission spectra of AVP and $[Asu^{1,6}]$AVP and absorption spectrum of cystine in buffer are shown in Fig. 3. The R_0 values were calculated based on integral spectral overlap, quantum yields (Asu-analogues, see Figs. 1 and 2) and orientation factor $\kappa^2 = 2/3$ (Förster 1948). To set a reasonable value of κ^2 in the case of intramolecular energy transfer has always been a problem and this has been discussed by Dale et al. (1979). We used a value of 2/3 which is an unweighted average over all orientations. This value is justified based on studies of the tyrosyl segmental rotational motion in oxytocin and vasopressin (Gryczynski et al. 1991). It was found that the rotational correlation time for tyrosyl in oxytocin and vasopressin (about 35 ps) is much shorter than the excited-state lifetimes of Asu-analogues (donors). It is likely that donors (tyrosyl residues) and acceptors (disulfide bonds) will achieve the isotropic distribution within tyrosyl lifetime scale. Additionally, NMR data suggest that in aqueous solution there is a considerable degree of flexibility in the backbone of oxytocin (Glickson et al. 1972). For high viscosity (P. G., –30 °C) the orientation factor was set as 0.474 (no rotational diffusion). The values of R_0 for each hormone at particular conditions are in Table 2. The energy transfer efficiencies can be calculted from the steady-state (I) or/and from intensity decay (I(t)) measurements

$$E_T = 1 - \frac{I_{DA}}{I_D}; \quad E_T = 1 - \frac{\int I_{DA}(t)dt}{\int I_D(t)dt} \tag{8}$$

Table 2. Energy transfer efficiencies determined from steady-state (S-S) and from frequency-domain intensity decays (F-D), distance distribution parameters, and Förster distances

Compound	Conditions	$E_T^{(S-S)}$	$E_T^{(F-D)}$	R_0(Å)	R_{av}(Å)	hw(Å)	$\chi^{2\,b}_R$
Arg^8-vasopressin	pH 7.0	0.65	0.63	8.24	7.51	2.63	7.6[b]
	pH 7.0	–	–	8.78[a]	8.00	2.80	7.6
	P. G., 40 °C	0.60	0.61	8.93	8.25	3.91	2.1
	P. G., –30 °C	0.53	0.45	9.11	9.54	3.36	2.7
	CHARMm	–	–	–	8.05	2.88	–
Oxytocin	pH 7.0	0.68	0.69	8.53	7.33	3.31	7.1
	pH 3.1	–	0.74	8.53	6.91	3.42	2.1
	pH 7.0	–	–	9.23[a]	7.94	3.58	7.1
	P. G., 40 °C	0.71	0.68	9.45	7.93	5.50	3.1
	P. G., –30 °C	0.67	0.63	9.34	8.17	6.12	4.7
	CHARMm	–	–	–	8.05	3.61	–

[a] Calculated using differential absorption spectrum (hormone – Asu-analogue)
[b] Goodness-of-fit from the distance distribution analysis (Eq. (6)) of the frequency-domain data

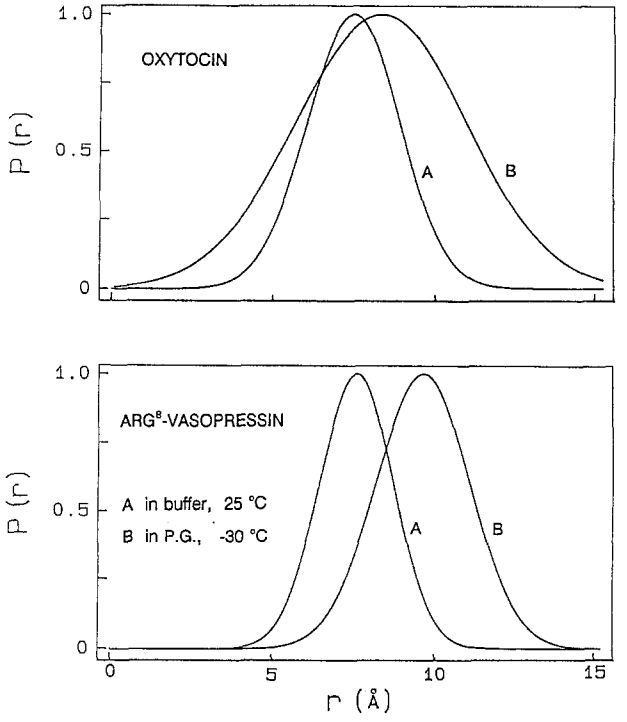

Fig. 4. Tyrosyl-to-disulfide distance distribution for oxytocin and [Arg^8]-vasopressin, *A* – in buffer (low viscosity); *B* – in propylene glycol at –30 °C (high viscosity) The distance distribution parameters in Table 1 were determined for the R_0 value calculated from the absorption spectrum of cystine

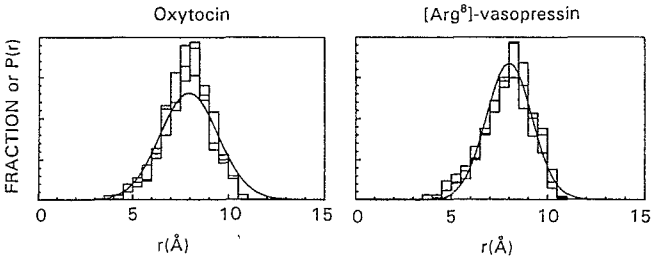

Fig. 5. Comparison of experimentally determined (*solid line*) and theoretically calculated (*histograms*) distance distribution profiles for oxytocin and Arg^8-vasopressin. The experimental distance distribution parameters are from Table 3 calculated using the differential (——) absorption spectra

where subscripts DA and D are for native and respective Asu-analogues, respectively. The energy transfer efficiencies determined from the steady-state measurements are in good agreement with those from frequency-domain intensity decays (Eq. (5)). The values are summarized in Table II. The quantum yields in buffer (pH 7) were determined as 0.026 for oxytocin and 0.081 for Asu^{1,6}-oxytocin. These data are in agreement with earlier cited values (Bodanszky et al. 1981; Ross et al. 1986 a). Similar values in buffer were obtained for AVP (0.021) and for [Asu^{1,6}]AVP (0.060).

To determine the distance distribution parameters (average distance, R_{av}, and half width of distance distribution, hw) intensity decays of native hormones were fitted to Eqs. (5–7). The values of α_{Di} and τ_{Di} are from respective Asu-analogues (see Table 1). The results of analyses of distance distribution are summarized in Table 2. In Fig. 4 are shown distance distribution for both hormones for low and high viscosity solvents. The larger value of the average distance (R_{av}) for AVP indicates a more extended conformation than for oxytocin. This observation is in agreement with earlier observations for oxytocin and vasopressin (Gryczynski et al. 1991). The distance distribution (hw) for AVP is narrower than for oxytocin (Table 2 and Fig. 4) which can be an effect of multicomponent distance distribution from three rotamer populations or less extensive diffusion. The analyes including diffusion coefficient were not performed because decay data alone were not adequate to yield both the distance distribution and the end-to-end diffusion coefficient (Lakowicz et al. 1991 a, b). The recovered distance distribution parameters also reflect unresolved multicomponent distance distributions from three rotamer populations.

We compared the experimentally recovered distance distribution parameters with those obtained from a molecular dynamics conformational survey using the program CHARMm with the parameter set form QUANTA 3.0

(Polygen Corp). The calculated distance distribution parameters (Table 2) were from an *in vacuo* molecular dynamics simulation consisting of 1500 steps as the result from 3 consecutive of 500 survey-steps. The predicted parameters from CHARMm are in satisfactory agreement with the experimentally determined parameters. Figure 5 shows a comparison of experimentally determined and calculated distance distribution parameters for both hormones. These experimental and theoretical agreements confirm that reduced fluorescence observed for the hormones, relative to their Asu-analogues, can be interpreted as a resonance energy transfer from the tyrosine residue to the disulfide bridge.

Acknowledgement. This work was supported grants from the National Institute of Health (GM 35 154 and GM 39 617), with support for the Center for Fluorescence Spectroscopy from the National Science Foundation (DIR-8 710 401 and DMB-8 804 931) and the National Institutes of Health (RR-08 119 and RR-07 510). JRL and WW also express appreciation for support from the Medical Biotechnology Center at the University of Maryland.

References

Bodanszky M, Tolle JC, Bednarek MA, Schiller PW (1981) Synthesis of 8-L-Tryptophan Oxytocin and Determination of one of Its Conformational Parameters. Int J Peptide Protein Res 17: 444–453

Brewster AIR, Hruby VJ (1973) 300-MHz Nuclear Magnetic Resonance Study of Oxytocin in Aqueous Solution: Conformational Implications. Proc Natl Acad Sci, USA 70: 3806–3809

Chen RF (1967) Fluorescence Quantum Yields of Tryptophan and Tyrosine. Anal Lett 1: 35–42

Cheung HC, Wang C-K, Gryczynski I, Malak H, Wiczk W, Johnson ML, Lakowicz JR (1991 a) Conformational Flexibility of the Cys 697–Cys 707 Segment of Myosin Subfragment-1: Distance Distribution by Frequency-Domain Fluorometry. Biophys Chem 40: 1–17

Cheung HC, Wang C-K, Gryczynski I, Wiczk W, Laczko G, Johnson ML, Lakowicz JR (1991 b) Distance distributions and anisotrophy decays of troponin C and its complex with troponin I. Biochemistry 30: 5238–5247

Cowgill RW (1964) Fluorescence and Structure of Proteins III. Effects of Denaturation on Fluorescence of Insulin and Ribonuclease. Arch Biochem Biophys 104: 84–92

Cowgill RW (1967) Fluorescence and Protein Structure XI. Fluorescence Quenching by Disulfide and Sulfhydryl Groups. Biochim Biophys Acta 140: 37–44

Craig LC, Harfenist EJ, Paladini AC (1964) Dialysis Studies VII. The Behavior of Angiotensin, Oxytocin, Vasopressin, and Some of Their Analogues. Biochemistry 3: 764–769

Dale RE, Eisinger J, Blumberg WE (1979) The Orientational Freedom of Molecular Probes. The Orientation Factor in Intramolecular Energy Transfer. Biophys J 26: 161–194

Eisinger J (1969) Intramolecular Energy Transfer in Adrenocarticotropin. Biochemistry 8: 3902–3908

Eisinger J, Feuer B, Lamola AA (1969) Intramolecular Singlet Excitation Transfer. Applications to Polypeptides. Biochemistry 8: 3908–3915

Förster TH (1948) Intermolecular Energy Migration and Fluorescence. Ann Phys (Leipzig) 2: 55–75 (Translation 1974 bs R. S. Knox)

Glickson JD, Urry DW, Havran RT, Walter R (1972) Proton Magnetic Resonance Comparison of Neurohypophyseal Hormones and Analogues: Deletion of Amino Groups and the Conformation of Lysine Vasopressin. Proc Natl Acad Sci USA 69: 2136–2140

Glickson JD, Urry DW, Walter R (1972) Method for Correlation of Proton Magnetic Resonance Assigment in Different Solvents: Conformational Transition of Oxytocin and Lysine Vasopressin from Dimethylsulfoxide to Water. Proc Natl Acad Sci USA 69: 2566–2569

Gratton E, Limkeman M, Lakowicz JR, Maliwal BP, Cherek H, Laczko G (1984) Resolution of Mixtures of Fluorophores Using Variable-Frequency Phase and Modulation Data. Biophys J 46: 479–486

Gryczynski I, Szmacinski H, Laczko G, Wiczk W, Johnson ML, Kusba J, Lakowicz JR (1991) Conformational Differences of Oxytocin and Vasopressin as Observed by Fluorescence Anisotropy Decays and Transient Effects in Collisional Quenching of Tyrosine Fluorescence. J Fluoresc 1(3): 163–175

Husain J, Blundell TL, Cooper S, Pitts JE, Ticle IJ, Wood SP, Hruby VJ, Buku A, Fischman AJ, Wyssbrod HR, Mascarenhas Y (1990) The Conformation of Deamino-Oxytocin: X Ray Analysis of the 'Dry' and 'Wet' Forms. Philos Trans R Soc Lond B 327: 625–654

Kraus EM, Cowburn D (1981) Hydrogen-Deuterium Exchange Kinetics of the Amide Protons of Oxytocin Studied by Nuclear Magnetic Resonance. Biochemistry 20: 672–679

Kusba J, Lakowicz JR (1994) Diffusion-Modulated Energy Transfer and Quenching; Analysis by Numerical Integration of the Diffusion Equation in LaPlace Space. In: Methods in Enzymology; Numerical Computer Methods, Part B, Vol. 242, Brand L, Johnson ML (eds) Academic Press, New York, pp 216–262

Langs DA, Smith GD, Stezowski JJ, Hughes RE (1986) Structure of Pressinoic Acid: The Cyclic Moiety of Vasopressin. Science 232: 1240–1242

Lakowicz JR, Laczko G, Cherek H, Gratton E, Limkeman M (1984) Analysis of Fluorescence Decay Kinetics from Variable-Frequency Phase Shift and Modulation Data. Biophys J 46: 463–477

Lakowicz JR, Laczko G, Gryczynski I (1986) 2 GHz frequency-domain fluorometer. Rev Sci Instrum 57: 2499–2506

Lakowicz JR, Gryczynski I, Cheung HC, Wang C-K, Johnson ML, Joshi N (1988) Distance Distributions in Proteins Recovered by Using Frequency-Domain Fluorometry. Applications to Troponin I and Its Complex with Troponin C. Biochemistry 27: 9149–9160

Lakowicz JR, Gryczynski I, Malak H, Wiczk W, Laczko G, Prendergast FC, Johnson ML (1990 a) Conformational Distributions of Melittin in Water/Methanol Mixtures from Frequency-Domain Measurements of Non-Radiative Energy Transfer. Biophys Chem 36: 99–115

Lakowicz JR, Wiczk W, Gryczynski I, Szmacinski H, Johnson ML (1990 b) Influence of end to-end diffusion on intramolecular energy transfer as observed by frequency-domain fluorometry. Biophys Chem 38: 99–109

Lakowicz JR, Kusba J, Szamcinski H, Gryczynski I, Eis PS, Wiczk W, Johnson ML (1991 a) Resolution of End to-End Diffusion Coefficients and Distance Distribution of Flexible Molecules Using Fluorescent Donor-Acceptor and Donor-Quencher Pairs. Biopolymers 31: 1363–1378

Lakowicz JR, Kusba J, Wiczk W, Gryczynski I (1991 b) Resolution of the Conformational Distribution and Dynamics of a Flexible Molecules using Frequency-Domain Fluorometry. Biophys Chem 39: 79–84

Laws WR, Ross JBA, Wyssbrod HR, Beechem JM, Brand L, Sutherland JC (1986) Time Resolved Fluorescence and ^{1}H NMR Studies of Tyrosine and Tyrosine Analogues: Correlation of NMR-Determined Rotamer Populations and Fluorescence Kinetics. Biochemistry 25: 599–607

Liwo A, Tempczyk A, Grzonka Z (1988) Molecular mechanics calculations on deaminooxytocin and on deamino-arginine-vasopressin and on its analogues. J Comput Aided Mol Des 2: 281–309

Polygen Corporation (1988) CHARMm 21.1.4 and Quanta Software. Polygen Corporation, Waltham, MA

Ross JBA, Laws WR, Buku A, Sutherland JC, Wyssbrod HR (1986 a) Time-Resolved Fluorescence and ^{1}H NMR Studies of Tyrosyl Residues in Oxytocin and Small Petides: Correlation of NMR-Determined Conformations of Tyrosyl Residues and Fluorescence Decay Kinetics. Biochemistry 25: 607–612

Ross JBA, Laws WR, Sutherland JC, Buku A, Katsoyannis PG, Schwartz IL, Wyssbrod HR (1986b) Linked-Function Analysis of Fluorescence Decay Kinetics: Resolution of Side-Chain Rotamer Populations of a Single Aromatic Amino Acids in Small Polypeptides. Photochem Photobiol 44: 365–370

Ross JBA, Laws WR, Rousslang KW, Wyssbrod WR (1992) Tyrosine Fluorescence and Phosphorescence from Proteins and Polypeptides. In: Topics in Fluorescence Spectroscopy; Biochemical Applications, Vol. 3. Lakowicz JR (ed). Plenum Press, New York, pp 1–63

Shafferman A, Stein G (1974) The Effect of Aromatic Amino Acids on the Photochemistry of a Disulfide Energy Transfer and Reaction with Hydrated Electrons. Photochem Photobiol 20: 399–406

Swadesh JK, Mui PW, Sheraga HA (1987) Thermodynamics of the Quenching of Tyrosyl Fluorescence by Dithiothreitol. Biochemistry 26: 5761–5769

Wood SP, Ticle IJ, Treharne AM, Pitts JE, Mascarenhas Y, Li JY, Husain J, Cooper S, Blundell TL, Hruby VJ, Buku A, Fischman AJ, Wyssbrod HR (1986) Crystal Structure Analysis of Deamino-Oxytocin: Conformational Flexibility and Receptor Binding. Science 232: 633–636